EXPERIMENTAL RESEARCH ON EFFECT OF HOOP REINFORCEMENT AND PARTIAL SLIT OF REINFORCED CONCRETE COLUMNS WITH SECONDARY WALLS

KOMURO Tatsuya[1], HIROSAWA Masaya[2], TSUKAMOTO Eiji[3]

[1] *Assistant to director, Structural Investigation Department, Center for Better Living, JAPAN*
[2] *Professor Emeritus, Dept. of Structural Engineering, Kogakuin University, JAPAN*
[3] *Building Investigation Diagnosis Center, Japan Association of Building Research Promotion, JAPAN*
Email: t-komurot@cbl.or.jp

ABSTRACT :

Authors report the test results of the 12 specimens of column with side walls and the 10 specimens of column with spandrel walls and hanging walls under repeated horizontal load with fixed axial force. Variables are spacing of hoop, existence of eccentric connection of secondary walls to a column, existence of partial slits between column and secondary walls and difference of load history. In this thesis, a secondary wall is a wall which attaches to the column which is inside a frame of a side wall, a spandrel wall and a hanging wall. Resultantly, the following items are made clear.

In case of the column with side walls, when the hoop ratio was high, it was sustained after the maximum capacity that the strength which larger than the simple sum of the strength of the column and the walls. However, when the hoop ratio was low, the strength deteriorated rapidly after the maximum capacity. This showed that the evaluation of the column with side walls could be estimated at two steps. Moreover, the maximum strength deteriorated about 1.6~16.3%, and was not observed the major change by eccentric connection of the side walls in the shear strength and the deformation performance. But, the difference was observed failure property, and the spiral shear crack occurred in the column where the secondary walls eccentric connected.

In case of the column with spandrel walls and hanging walls, it becomes the short column and causes brittle shear failure. And when especially the hoop ratio was low, the maximum strength was deteriorated rapidly. In addition, the maximum strength deteriorated about 9%~25% with effect of the torsion moment with eccentric connection.

When the partial slit was used in the secondary walls of the column with side walls, spandrel walls and hanging walls, ductility performance of the column was improved, and the reinforcement effect has been verified.

Lastly, although the strength can be presumed under some deviation from the existing valuation estimation methods, failure mode can be hardly presumed.

KEYWORDS:
Column with Side Walls, Column with Spandrel/Hanging Walls, Hoop Ratio, Eccentric Connection, Partial Slit

1. PURPOSE

In an existing reinforced concrete structure, short columns having non-structural walls give significant impacts on the seismic performance of the system as a whole. This study focuses on such short columns, particularly those with non-structural walls eccentric to the column axis (hereinafter, "Eccentric Non-Structural Walls"), which currently lack sufficient experimental or engineering data despite the popular applications, and clarifies how columns with sidewalls and those with hanging/podium walls eccentric to the column axis behave until they undergo large deformation. In addition, the effect of structural slits on the brittle behavior of short columns is examined through tests on specimens with and without such slits. It should be noted that the structural slits examined here are limited to partial ones that allow in-service retrofitting. Based on the results of these tests, this study aims to further rationalize the seismic evaluation and seismic retrofit design for existing reinforced concrete structures.

2. Outline of the Tests

In this study, short columns of a axial stress of 30kgf/cm2 (partially 60kgf/cm2) and a hoop reinforcement ratio of approximately 0.1 to 0.2% having the following walls on both sides were designated as the standard short columns with non-structural walls in relatively old low- to medium-rise buildings: sidewalls twice as long as the column depth; and hanging/podium walls having an internal length of 1.5 times longer than the column depth. The specimens were subjected to static cyclic loading under a constant axial force. One of the objectives of these tests included the confirmation of vertical load-bearing capacity after the horizontal strength started to decrease. The specimens consisted of the following, categorized by variable factor, e.g. configurations:

Specimen configurations: 16 specimens with sidewalls and 14 with hanging/podium walls.

Presence of slits: 16 specimens with slits (2 with a deeper slit depth) and 14 without.

Hoop reinforcement ratio: 15 specimens at 0.1% and 15 at 0.26%.

Alignment of the non-structural walls in relation to the column axis: 22 specimens with eccentric walls and 8 with concentric ones.

Axial stress: 22 specimens with 0.1 Fc and 8 with 0.2 Fc.

Loading cycles: 26 specimens subjected to a large number of cycles and 4 to a small number of cycles.

2.1. Outline of the Specimens

(1) Columns and non-structural walls

The specimens were created on a scale of 1 to 2.5 due to test machinery constraints; the sectional dimensions and wall thickness were reduced from 60cm to 24cm and 12cm to 5cm, respectively. The hoop spacing was reduced from 25cm to 10cm for the columns of the Phase I (before 1970) and 10cm to 4cm for those of the Phase II (1971 to 1980). Wall reinforcement intervals were reduced from 25cm to 10cm for both phases. Reinforcing bars of 10-D10 (p_g = 1.24%), 4-D10 (p_t = 0.50%) and 4φ were used as the main reinforcement of the columns, main tensile and wall reinforcement and hoops, respectively. These were common to columns with sidewalls (hereinafter, the “CSW Series”) and those with hanging/podium walls (hereinafter, the “CHW Series”). The non-structural walls of both Series were basically situated eccentric to the column axis.

(2) Structural slits

For an approximately half of the specimens of both Series, full-length structural slits were provided at joints between the non-structural walls and columns (Figs. 1a and 1b). They were all partial ones, basically with a width (t_s) of 15mm and a depth (t_d) of 25mm (1/2 of the wall thickness), except two of the CHW Series that had a slit depth of td = 37.5mm (3/4 of the wall thickness).

(3) Columns with sidewalls (The CSW Series)

Figure 1a and Table 1a show specimen configurations and a list of all the 16 specimens, respectively. Every specimen had a height (h) of 100cm and a length (l_w) of 120cm. Designated as variable factors were: the alignment of walls in relation to the column axis (12 eccentric and 4 concentric), hoop reinforcement ratio (8 with p_w = 0.105% and 8 with p_w = 0.26%), presence of slits (8 with and 8 without) and loading history (12 subjected to a large number of cycles and 4 subjected to a small number of cycles).

(4) Columns with hanging/podium walls (The CHW Series)

Figure 1b and Table 1b show specimen configurations and a list of all the 14 specimens, respectively. Every specimen had a hanging wall height (HWL) of 24cm, a podium wall height (HHD) of 40cm and an internal column height (h_0) of 36cm. The columns were of the short type where h_0/D_c = 1.5. Designated as variable factors were: the alignment of walls in relation to the column axis (10 eccentric and 4 concentric), hoop reinforcement ratio (7 at 0.105% and 7 at 0.26%), and the presence and depth of slits (6 with slits of t_d/t_w = 1/2, two with slits of t_d/t_w = 3/4, and 6 without any slits).

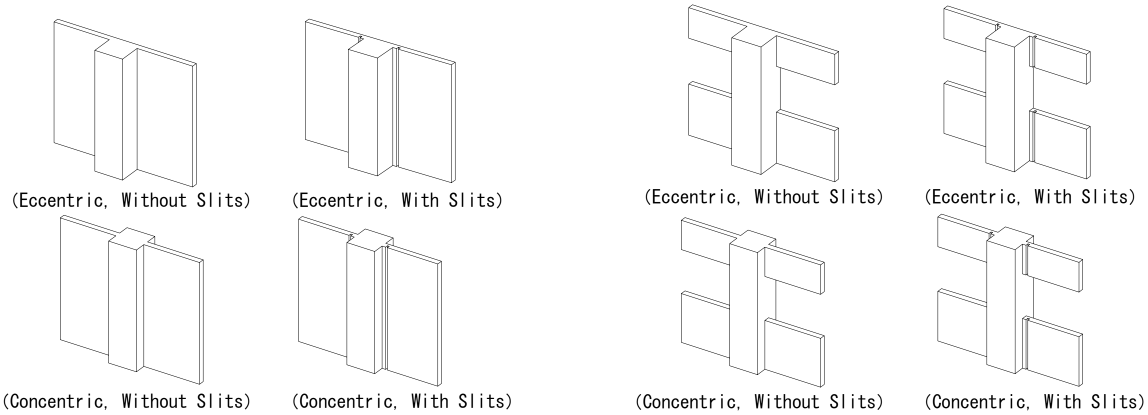

a) Column with side walls   b) Column with spandrel/hanging walls

Fig. 1 Specimen configuration

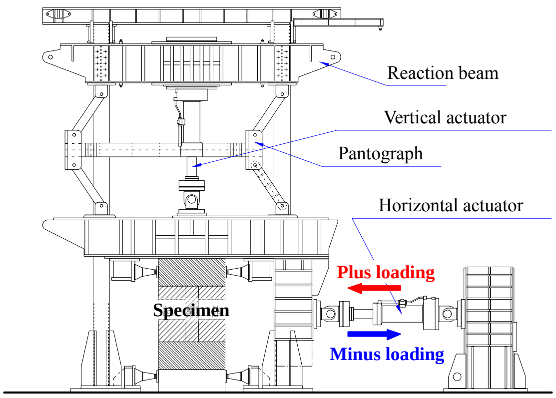

Fig. 2 The loading device of Column

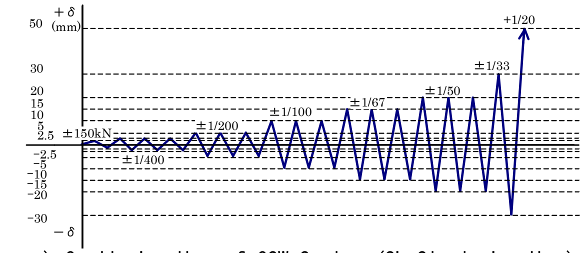

a) Cyclic Loading of CSW Series (SL:Simple Loading)

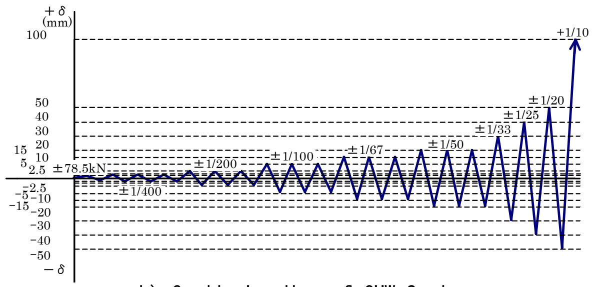

b) Cyclic Loading of CHW Series

Fig. 3 Horizontal loading history

(5) Materials

The average compressive strength of concrete used for all the specimens was approximately 270kgf/cm^2. The yielding points of reinforcing bars were approximately 3700kgf/cm^2 and 4800kgf/cm^2 for the main reinforcement (D10) and hoops (4φ), respectively.

(6) Axial loading

An axial load of approximately 0.1Fc (30kgf/cm^2) in column section area equivalent was applied to the 12 specimens having sidewalls (The CSW Series) in the second year and to the 10 specimens having hanging/podium walls (The CHW Series) in the third year. For 4 specimens each of the CSW and CHW Series in the fourth year, the axial load was set at approximately 0.2Fc to study the impact of the scale of axial force. The column loading device developed by the Building Research Institute was employed here, where the upper and lower stubs were restrained with a pantograph to keep parallel shifts in the horizontal direction, as shown in Fig. 2. The top of the vertical actuator was connected to the loading frame via roller bearings. The relative horizontal displacements of the upper and lower stubs were measured, and the measured value was then divided by the material length of the column. The resultant value was defined as the joint translation angle R. With regard to the loading history, the specimens were subjected to a large number of alternating horizontal cyclic loading under a constant axial force of 339.0 KN (η = 0.2) with the horizontal actuator. The load was applied until the columns were crushed and shrunk by 30mm or more in the vertical direction. The loading was forcibly terminated upon reaching that point.

(7) Horizontal loading history

All the specimens of both Series were basically subjected to a large number of static cycling loading in the horizontal direction, as shown in Fig. 3. For the CSW Series, the cycling loading was applied mainly with a joint translation angle of 1/400 to 1/50, which was terminated when the horizontal strength was reduced to approximately 20% of the maximum strength. For the CHW Series, horizontal cyclic loading was applied with a joint translation angle of 1/400 to 1/50 until the columns were finally crushed in the vertical direction.

Table 1a List of the CSW series

Year	Number	Specimen name	Hoop ratio (%)	Slit	Eccentric	Load history	Axial stress
2002	No. 1	01C10EW-CL	0.10	without	with	CL	0.11
	No. 2	02C10EW-SL		without		SL	
	No. 3	03C10EWSCL		with		CL	
	No. 4	04C10EWSSL		with		SL	
	No. 5	05C04EW-CL	0.26	without		CL	
	No. 6	06C04EW-SL		without		SL	
	No. 7	07C04EWSCL		with		CL	
	No. 8	08C04EWSSL		with		SL	
	No. 9	09C10CW-CL	0.10	without	without	CL	
	No. 10	10C10CWSCL		with			
	No. 11	11C04CW-CL	0.26	without			
	No. 12	12C04CWSCL		with			
2004	No. 13	01C10EW-	0.10	without	with	CL	0.21
	No. 14	02C10EWS1/2		with			
	No. 15	03C04EW-	0.26	without			
	No. 16	04C04EWS1/2		with			

【Common Factor】
Column section: $b_c \times D_c$=240mm×240mm, Main reinforcement ratio: p_g=1.24%(10-D10), Tensile reinforcement ratio: p_t=0.49%(4-D10), Wall thickness: t_w=50mm, Length of one side walls: l_w=480mm, Wall thickness ratio: $\alpha=0.21(=t_w / b_c)$,
Overhanging ratio of depth to Compression/Tension side: $\beta_c=2.00, \beta_t=2.00(=l_w / D_c)$, Vertical/Horizontal reinforcement: 1-4φ@100(Reinforcement ratio: p_s=0.26%), Axial stress ratio: $\eta=\sigma_0/\sigma_B$=0.11and 0.21, Axial stress of column: $\sigma_0=N/(b_c \times D_c)$=2.95 or 5.89N/mm^2

Table 1b List of CHW Series

Year	Number	Specimen name	Hoop ratio (%)	Slit	Slit Depth	Eccentric	Load history	Axial stress
2003	No. 1	01C10EW-	0.10	without	—	with	CL	0.11
	No. 2	02C10EWS1/2		with	1/2			
	No. 3	03C10EWS3/4		with	3/4			
	No. 4	04C04EW-	0.26	without	—			
	No. 5	05C04EWS1/2		with	1/2			
	No. 6	06C04EWS3/4		with	3/4			
	No. 7	07C10CW-	0.10	without	—	without		
	No. 8	08C10CWS1/2		with	1/2			
	No. 9	09C04CW-	0.26	without	—			
	No. 10	10C04CWS1/2		with	1/2			
2004	No. 11	01C10EW-	0.10	without	—	with		0.21
	No. 12	02C10EWS1/2		with	1/2			
	No. 13	03C04EW-	0.26	without	—			
	No. 14	04C04EWS1/2		with	1/2			

【Common Factor】
Column section: $b_c \times D_c$=240mm×240mm, Main reinforcement ratio: p_g=1.24%(10-D10)
Tensile reinforcement ratio: p_t=0.49%(4-D10), Wall thickness: t_w=50mm,
Internal dimension of column: h_0=360mm, h_0/D=1.5
Width-thickness ratio: $\alpha=0.21(=t_w/b_c)$, Overhang ratio: β=2.0(=lw/Dc), Vertical reinforcement: 4φ@100(Reinforcement ratio: p_{sv}=0.26%), Axial stress ratio of column: $\eta=\sigma_0/\sigma_B$=0.11 or 0.21, Axial stress of column: $\sigma_0=N/(b_c \times D_c)$=2.95 or 5.89N/mm^2

3. Results

3.1 Test Results Summary

On the whole, the strength, deformation performance and limit axial load-bearing capacity of the specimens were significantly affected by the presence of structural slits and the axial load levels and hoop reinforcement ratio of the columns. On the other hand, the eccentricity of non-structural walls to the column axis and the loading history (number of cycles) had a little impact. In other words, all the CSW and CHW specimens without structural slits underwent diagonal shear failure, and while they showed the higher maximum strength than that of the specimens having slits, they failed with small horizontal joint translation angles. The CSW and CHW specimens having slits, on the other hand, experienced shear failure at the slits, and while their maximum strength decreased, the effective length of the columns became longer, and the columns' own bending strength was maintained until the distortion angle became relatively large.

The effects of structural slits in improving deformation performance described above were significant in the Phase-II columns having a slightly higher hoop reinforcement ratio. By contrast, the deformation performance of the Phase I specimens having a smaller p_w was not improved much in this regard.

The eccentricity of the walls did not affect the strength, deformation performance and failure modes. However, it was found that the CSW specimens with concentric walls and structural slits showed lower strength as the slits failed at an early stage, and that the Phase-II columns with eccentric walls showed a slight torsion influence in the failure mode, as compared with those with concentric walls. While loading history did not have significant impacts, slightly larger joint translation angles were observed where the number of cycles was small.

3.2 Test Results for Columns with Sidewalls (the CSW Series)

(1) Failure process

Figures 4a, 4b, 4c and 4d show some of the test results for the CSW Series. Figures 4a and 4c show how the presence of structural slits influenced the relationship between shear force and joint translation angle (*Q-R* curve) and how the failure progressed in the Phase-I CSW Series (i.e. Specimens Nos. 1 & 3 and 13 & 14). Figures 4b and 4d show the same data for the Phase-II CSW Series (i.e. Specimens Nos. 5 & 7 and 15 & 16). The crack diagrams show that the specimens without structural slits developed diagonal cracking before undergoing failure. There are not much difference in cracking conditions between the eccentric (south) side and the concentric (north) side. On the other hand, those with structural slits, which are shown on the right hand side of the figures, underwent failure at the slits as early as at R = 1/200. The non-structural walls did not undergo shear failure until they developed a large deformation; they were separated from the columns and underwent bending failure, while the columns underwent shear failure after the bending yield, followed by a reduction in the strength. It should be noted that although Specimens Nos.5 and 15 had no structural slits, they displayed similar behaviors as those of Nos.7 and 16 having slits; their failure modes and *Q-R* curves were found to be in the intermediate range.

(2) Strength and deformation performance

Figures 5a and 5b show envelops of eight CSW specimens, including those with σ_0 = 30kgf/cm^2.

Where the axial force ratio was 0.2 or 0.1, the presence of slits slightly reduced the maximum strength, and those without slits showed a greater rate of decrease in strength than those with slits. On the other hand, those with slits lost strength more slowly even after reaching the maximum strength. This is due to the fact that where there were no slits; the whole system including sidewalls underwent shear failure. By contrast, where slits were provided, they were cut off from the system and let the sidewalls undergo bending failure together with the columns.

The difference in the hoop reinforcement ratio did not have significant impacts on the maximum strength, but did affect the post-maximum strength behaviors. It was found that the higher the hoop reinforcement ratio, the smaller the rate of reduction in strength.

The impact of axial force ratio on the maximum strength was approximately 5%; strength was not increased much by an increase in axial force. When η became large, it had extreme impacts on the post-peak strength reduction.

(3) Limit axial load-bearing capacity

Figure 6 shows the relationship between the shear force and joint translation angle upon reaching the maximum strength, i.e. Q_{max} and R_{Qmax}, respectively, and those upon reaching the limit axial load-bearing capacity, i.e. Q_u and R_u, respectively. The shear forces are represented by absolute values. For the CSW Series with η = 0.1, the value of R_u is an estimation. Q_u is not shown. The following insights were gained here:

The value of R_u was approximately twice to ten times greater than R_{Qmax} without slits.

The value of R_u of those with slits was approximately twice that of those without.

The higher the axial force ratio, the smaller the value of R_u. Where p_w = 0.26%, in particular, the value of R_u with η = 0.2 was less than a half of that with η = 0.1.

The value of R_u with η = 0.1 is expected to increase further. Also, where η = 0.1, provision of slits will give the same effect as those with η = 0.2 with slits.

Where η = 0.1, failure in the axial direction usually occurred under a newly experiencing large deformation. Where η = 0.2, on the other hand, such failure often occurred while undergoing an already experienced deformation during cyclic loading. This is due to the fact that the large axial caused concrete failure to progress during the repeated loading.

(4) Energy absorption performance

Figure 7 shows the sum total area of hysteresis loop (ΔW) during the cyclic loading on each specimen. The simple comparison of the area of hysteresis loop up to the limit axial load-bearing capacity revealed the following:

The value of ΔW was significantly varied by different hoop reinforcement ratios. The average value of ΔW of Phase-II columns (p_w = 0.26%) was approximately 1.87 times greater than that of the Phase-I columns (p_w = 0.10%), indicating that the Phase-II columns were highly ductile.

Provision of partial slits slightly increased the amount of energy absorbed; where η = 0.2, the amount of energy absorbed in No.14 was 3.19 times greater than that in No.13, while that in No.16 was 1.45 times greater

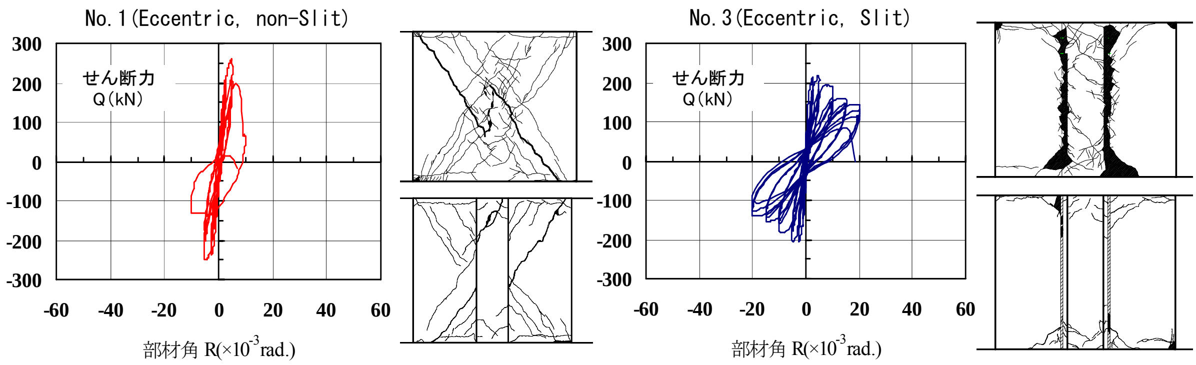

Fig. 4a Q—R Curve of Column with side walls(Phase-Ⅰ)・Crack diagram (p_w=0.10%、σ_0=30kgf/cm^2)

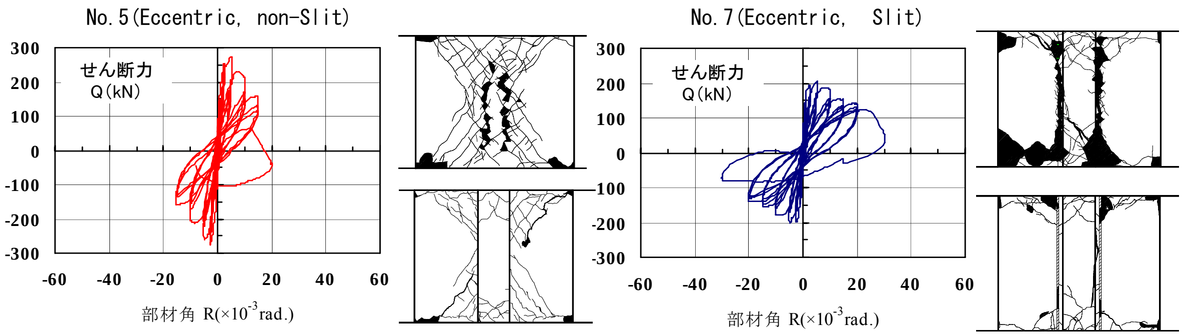

Fig. 4b Q—R Curve of Column with side walls(Phase-Ⅱ)・Crack diagram (p_w=0.26%、σ_0=30kgf/cm^2)

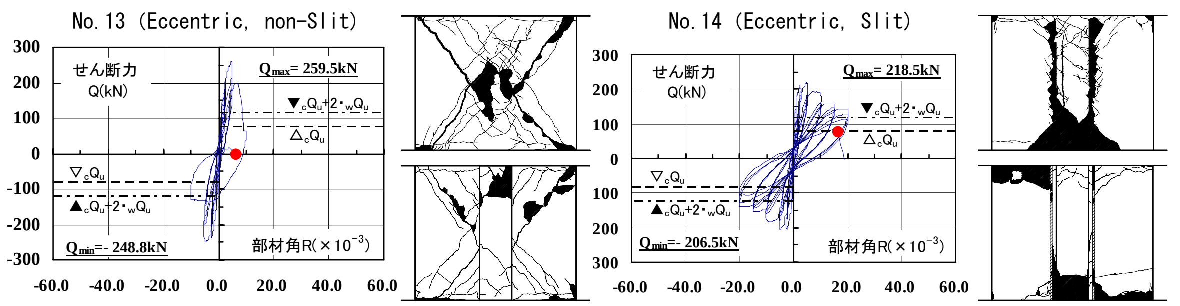

Fig. 4c Q—R Curve of Column with side walls(Phase-Ⅰ)・Crack diagram (p_w=0.10%、σ_0=60kgf/cm^2)

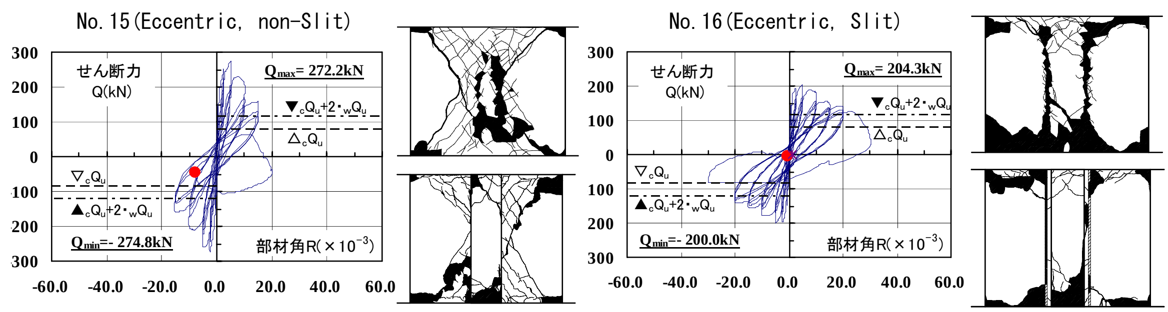

Fig. 4d Q—R Curve of Column with side walls(Phase-Ⅱ)・Crack diagram (p_w=0.26%、σ_0=60kgf/cm^2)

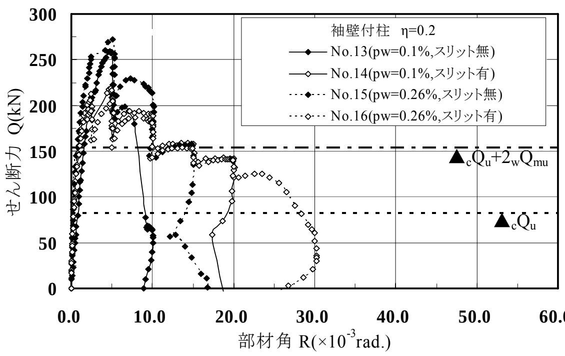

Fig.5a Envelope Curve (CSW series, η=0.2)

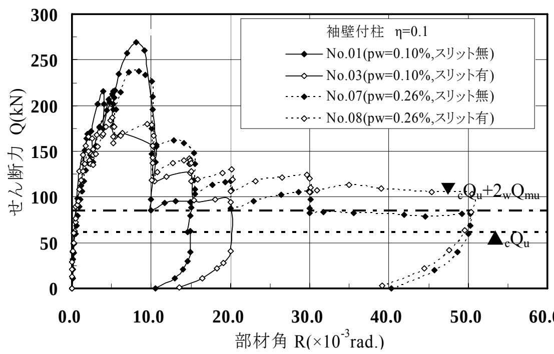

Fig.5b Envelope Curve(CSW series, η=0.1)

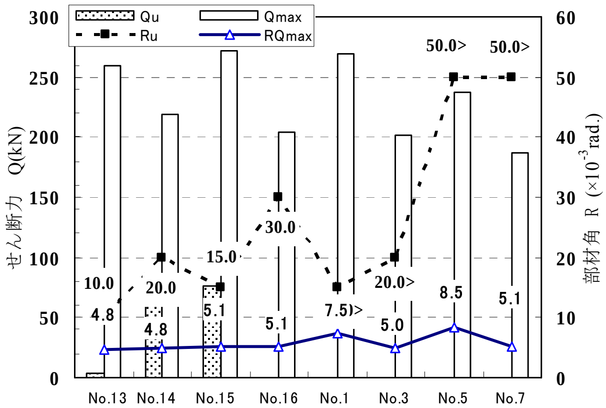

Fig.6 Relationship between the shear force and deflection angle upon reaching the maximum strength

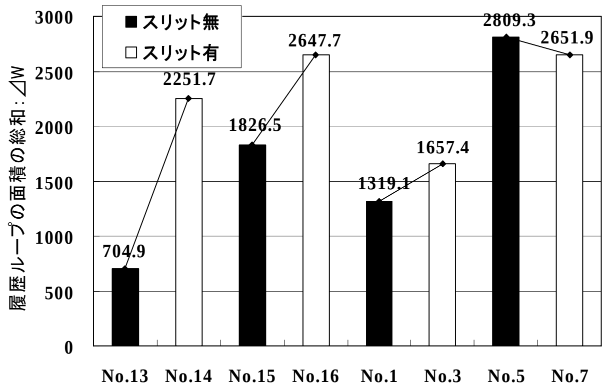

Fig.7 Summation of Hysteresis loop (⊿W)

than that in No.15. Where partial slits were provided, the Phase-I columns showed a greater rate of increase in the amount of energy absorbed.

The increase in the axial force ratio reduced the energy absorption performance; where there were no slits, the energy absorption performance in the case of η = 0.2 was 0.53 times and 0.65 times less than that in the case of η = 0.1 where p_w = 0.10% and p_w = 0.26%, respectively. Where slits were provided, the energy absorption performance in the case of η = 0.2 was 1.36 times greater than and the same as that with η = 0.1 where p_w = 0.10% and pw = 0.26%, respectively. The reason for the amount of energy absorbed being greater in those having slits and in the case of η = 0.2 is because the final loading applied in the η = 0.1 tests was set at 20% of the maximum strength or less.

(5) Examination of the ultimate strength

Table 2 shows the results of the ultimate strength analysis. For the columns with sidewalls, their ultimate bending and shear strengths were calculated using the existing evaluation formulas, which were then compared with the test data. The ultimate strength of the columns without any sidewalls and that of two self-supporting sidewalls without a column were also calculated and compared. When calculating the ultimate strength of specimens with slits, they were treated as having a uniform thickness, which was obtained by deducting the depth of the slits (t_s = 25mm) from the wall thickness (t_w = 50mm).

In the tests, shear failure of sidewalls was first observed, followed by the shear failure of the columns. The calculation results for the ultimate shear strength (${}_{cw}Q_{su}$) were found to be quite similar to the test results, i.e. 0.98 to 1.2 of the test results. However, the failure mode was found to be more complicated; it was difficult to distinguish between bending failure, shear failure and the failure of sidewall-column interfaces, and thus it was not straightforward to estimate them with the evaluation formulas.

Where slits were provided, they detached the sidewalls from the columns by failing. The two sidewalls underwent bending or bending crushing with a shear-bending capacity ratio (S_w) of 2.11, while the columns first experienced the bending yield at the top and base and then underwent shear failure. Here also, it was found difficult to estimate the failure mode with the evaluation formulas. Nonetheless, an approximately similar value for the maximum strength was obtained by replacing tw in Equation (2) with tw', i.e. the wall thickness less the slit depth as shown in Equation (5), in calculating the ultimate shear strength.

$$t_w' = t_w - t_d \quad \cdots\cdots\cdots\cdots \quad (5)$$

where, t_w: sidewall thickness and td: depth of partial slits

Table 3 Comparison the test and calculation results (CSW series)

No	Specimen name	Test value				Calculation value									Test/Calculation	
						Columns with side walls			Independent columns			Side wall(Two wall)				
		Load direction	$_tQ_{max}$ (kN)	R_{Qmax} (10^3rad.)	Failure mode	$_{cw}Q_{mu}$ (kN)	$_{cw}Q_{su}$ (kN)	S_{cw}	$_cQ_{mu}$ (kN)	$_cQ_{su}$ (kN)	S_c	$_wQ_{mu}$ (kN)	$_wQ_{su}$ (kN)	S_w	$_tQ_{max}/_{cw}Q_{mu}$	$_tQ_{max}/_{cw}Q_{su}$
13	01C10EW−	Plus	259.6	4.770	WS→CS(DT)	492.20	215.46	0.44	82.09	103.28	1.26	71.61	93.90	1.31	0.53	1.20
		Minus	-248.8	-4.485											0.51	1.15
14	02C10EWS1/2	Plus	218.5	4.835	ST→WB,CS	466.77	185.78	0.40							0.47	1.18
		Minus	-206.6	-5.005											0.44	1.11
15	03C04EW−	Plus	272.2	5.040	WS→CS	492.20	236.29	0.48		115.96	1.41				0.55	1.15
		Minus	-274.9	-2.510											0.56	1.16
16	04C04EWS1/2	Plus	204.3	5.050	ST→WFC,CS	466.77	204.08	0.44							0.44	1.00
		Minus	-200.0	-4.980											0.43	0.98

注) $_tQ_{max}$: Maximum shear force of the test　　R_{Qmax} : Deflection angle when maximum shear force

$_{cw}Q_{mu}$: Bending ultimate strength of Column with side walls (by (1) formula)　　$_{cw}Q_{su}$: Shear ultimate of Column with side walls (by (2) formula)

$_cQ_{mu}$: Bending ultimate strength of Column (by (3) formula)　　$_cQ_{su}$: Shear ultimate of column (by (4) formula)

$_wQ_{mu}$: Bending ultimate of side walls(by (3) formula)　　$_wQ_{su}$: Shear ultimate of side wall (by (4) formula)

S_{cw} : Safety factor of column with side walls $_{cw}Q_{mu}/_{cw}Q_{su}$　　S_c : Safety factor of independent column $_cQ_{mu}/_cQ_{su}$

S_w : Safety factor of side walls $_wQ_{mu}/_wQ_{su}$

$$_{cw}M_u = (0.9+\beta)\ a_t\cdot\sigma_y\cdot D + 0.5N\cdot D\left\{1+2\beta-\frac{N}{b_e\cdot D\cdot\sigma_B}\left(1+\frac{a_t\cdot\sigma_y}{N}\right)^2\right\} \rightarrow {}_{cw}Q_{mu} = \frac{2\,{}_{cw}M_u}{h_0} \quad \cdots (1)$$

$$_{cw}Q_{su} = \left\{\frac{0.092k_u k_p(180+\sigma_B)}{M/(Q\cdot d_e)+0.12} + 2.7\sqrt{p_w\cdot{}_s\sigma_{wy}\left(\frac{b}{b_e}\right) + p_{sh}\cdot{}_s\sigma_{yh}\left(\frac{t_w}{b_e}\right)}\right\} b_e\cdot j_e + 0.1N \quad \cdots (2)$$

$$_cM_u = 0.8\ a_t\cdot\sigma_y\cdot D + 0.5N\cdot D\left(1-\frac{N}{b\cdot D\cdot\sigma_B}\right) \rightarrow {}_cQ_{mu} = \frac{2\,{}_cM_u}{h_0} \quad \cdots (3)$$

$$_{cw}Q_{su} = \left\{\frac{0.12k_u\cdot k_p(180+\sigma_B)}{M/(Q\cdot d)+0.12} + 2.7\sqrt{p_w\cdot{}_s\sigma_{wy}}\right\} b\cdot j + 0.1N \quad \cdots (4)$$

Failure mode : Capacity→Ductility　　( ): Unclear mode

CS : Shear failure of column　　DT: Diagonal shear wall　　WS: Shear failure of side walll

WFC : Bending crushing of side wall　　WB: Bending crushing of side wall　　ST: Slit failure

3.3 *Test Results for Hanging/Podium Walls (the CHW Series)*

(1) Failure process

Figures 8a, 8b, 8c and 8d show some of the test results for the CHW Series. Figures 8a and 8c show how the presence of structural slits influenced the *Q-R* curve and how the failure progressed in the Phase-I CHW Series (Specimen Nos. 1 & 2 and 11 & 12). Figures 9b and 9d show the same data for the Phase-II CHW Series (Specimen Nos. 4 & 5 and 13 & 14). The cracking and failure conditions indicate that the short columns having hanging/podium walls without structural slits (Specimen Nos. 1 & 4 and 11 & 13) shown on the left hand side of the figures underwent diagonal shear failure with a small joint translation angle (R≈1/200), experiencing an extreme strength reduction. On the other hand, those with slits (Specimen Nos. 2 & 5 and 12 & 14) shown on the right hand side of the figures started to fail at the slits at R = 1/200, followed by bending yield as long columns, and withstood until a large deformation of R = 2/100 to 4/100 without experiencing a significant strength reduction. When compared in terms of the value of p_w (Specimen Nos. 1 & 4, 2 & 5 and 11 & 14), those with p_w = 0.26% showed all better deformation performance; in particular, those with slits were found to be more ductile.

(2) Strength and deformation performance

Figure 10 shows envelops of eight CHW specimens, including those with $\sigma_0 = 30\text{kgf/cm}^2$.

Where the axial force ratio η = *0.2*, the presence of slits did not affect the maximum strength much, but gave significant impacts on the deformation performance. Where there were no slits, a significant reduction in strength was observed under cyclic loading after reaching the maximum strength. The specimens having slits, on the other hand,

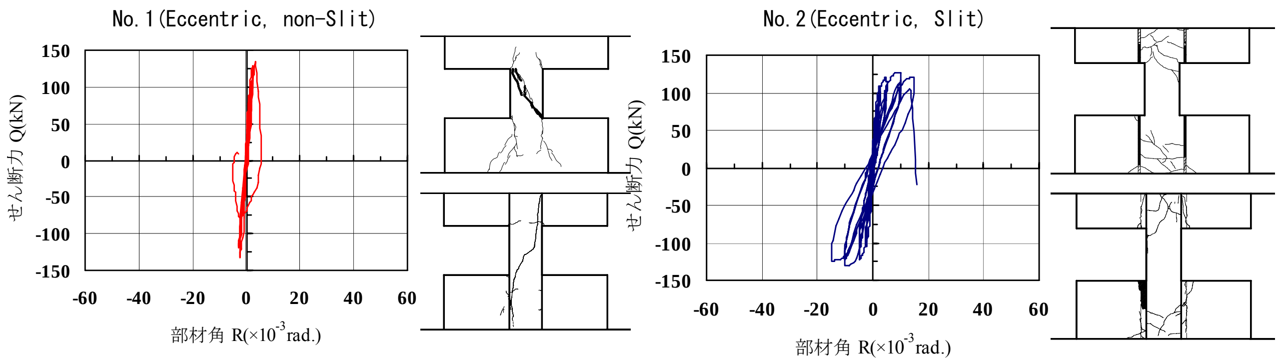

Fig. 8a Q-R Curve of CHW series (Phase-Ⅰ) · Crack diagram (p_w=0.10%、σ_0=30kgf/cm^2)

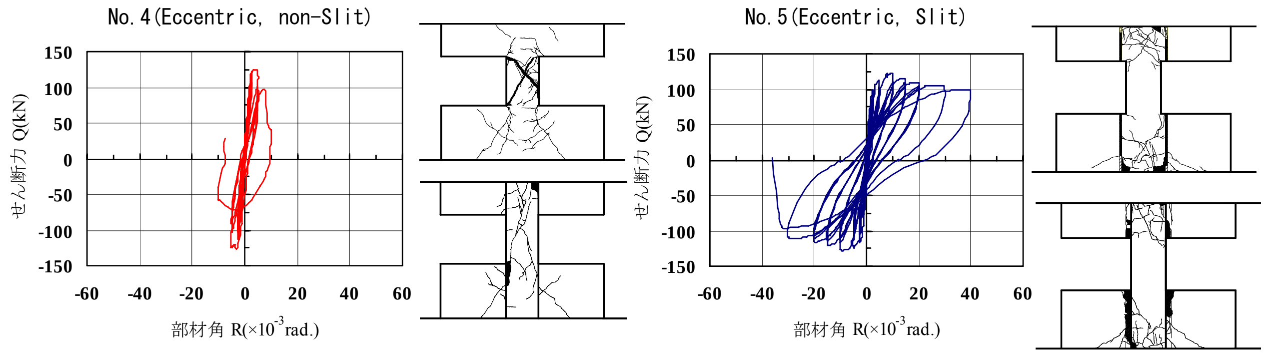

Fig. 8b Q-R Curve of CHW series (Phase-Ⅱ) · Crack diagram (p_w=0.26%、σ_0=30kgf/cm^2)

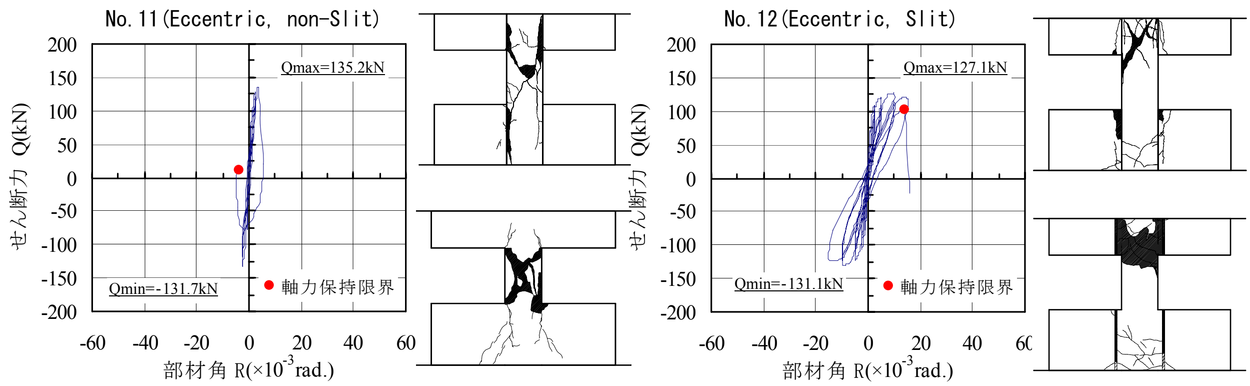

Fig. 8c Q-R Curve of CHW series (Phase-Ⅰ) · Crack diagram (p_w=0.10%、σ_0=60kgf/cm^2)

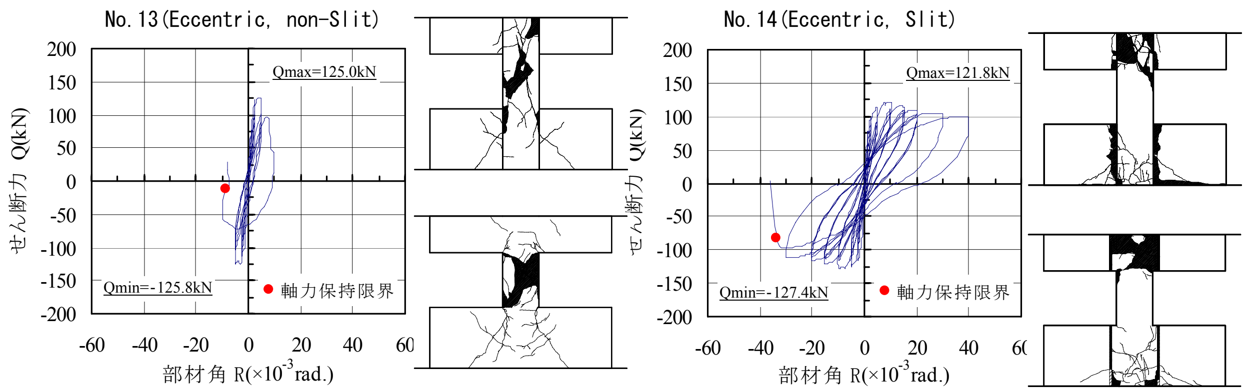

Fig. 8d Q-R Curve of CHW series (Phase-Ⅱ) · Crack diagram (p_w=0.26%、σ_0=60kgf/cm^2)

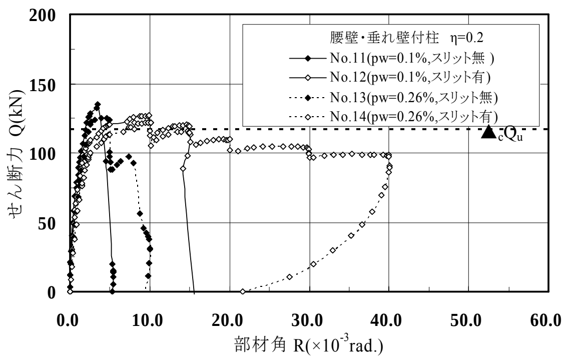

Fig. 9a Envelope Curve (CHW series, η=0.2)

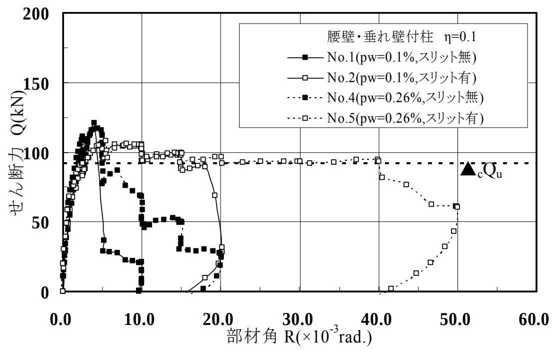

Fig. 9b Envelope Curve (CHW series, η=0.1)

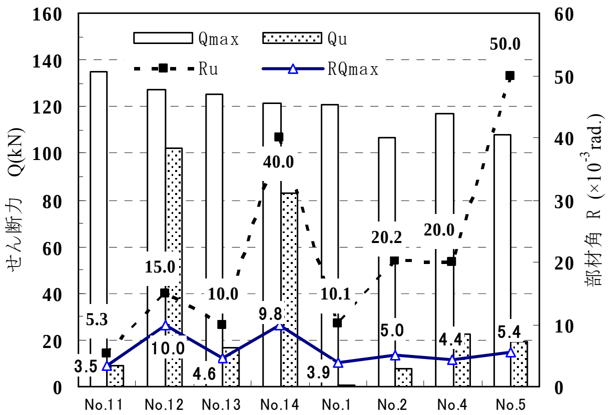

Fig. 10 Relationship between the shear force and deflection angle upon reaching the maximum strength

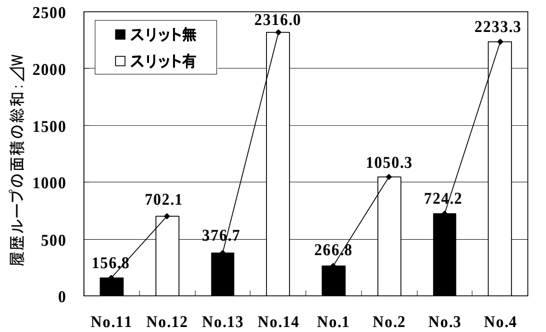

Fig. 11 Summation of Hysteresis loop (⊿W)

experienced a reduction to a much lesser extent; the strength decreased at a slower rate after reaching the maximum strength. This tendency was more obvious where the axial force ratio $\eta = 0.1$.

The height of hoop reinforcement ratio did not affect the maximum strength much, but did have significant impacts after reaching the maximum strength.

With regard to the axial force ratio, the maximum strength was affected slightly more in the case of $\eta = 0.2$ than in the case of $\eta = 0.1$. It was also found that the greater the value of η, the more significant the impacts on the post-maximum strength reductions. However, where slits were provided, the value of η did affect the joint translation angle upon reaching the limit axial load-bearing capacity although the strength showed similar reduction tendencies.

(3) Limit axial load-bearing capacity

For the CHW Series, Figure 11 shows the relationship between the shear force and joint translation angle upon reaching the maximum strength, i.e. Q_{max} and R_{Qmax}, respectively, and those upon reaching the limit axial load-bearing capacity, i.e. Qu and Ru, respectively. The shear forces are represented by absolute values.

The value of Ru was approximately 1.5 to 9.2 times greater than R_{Qmax} without slits, showing a higher rate of increase in the case of $\eta = 0.1$.

The value of R_u of those with slits was twice to 4 times greater than that of those without.

The value of R_u where the hoop reinforcement ratio $p_w = 0.26\%$ was approximately twice that in the case of $p_w =$ 0.10%.

The higher the axial force ratio, the smaller the value of R_u, which became approximately 0.5 times less where there were no slits, and 0.75 to 0.8 times less where slits were provided.

Axial collapsing usually occurred under a newly experiencing large deformation in the case of $\eta = 0.1$. Where $\eta = 0.2$, on the other hand, such failure often occurred while undergoing an already experienced deformation during cyclic loading. This is due to the fact that the large axial force caused concrete failure to progress during the repeated loading.

The value of Q_u bore the axial force up to a point where the horizontal force neared zero in the case of $\eta = 0.1$ and $\eta = 0.2$ without slits. However, in the case of $\eta = 0.2$ having slits, it rapidly became impossible to bear the axial force although adequate horizontal strength was still retained.

(4) Energy absorption performance

Figure 12 shows the sum total area of hysteresis loop (ΔW) during the cyclic loading on each specimen. The simple comparison of the area of hysteresis loop up to the limit axial load-bearing capacity revealed the following:

The value of ΔW was significantly varied by different hoop reinforcement ratios. The average value of ΔW of Phase-II columns ($pw = 0.26\%$) was approximately 2.47 times greater than that of the Phase-I columns ($pw = 0.10\%$), indicating that the Phase-II columns were highly ductile.

Provision of partial slits did increase the amount of energy absorbed; where $\eta = 0.2$, the amount of energy absorbed in No.12 was 4.48 times greater than that in No.11, while that in No.14 was 6.15 times greater than that in No.13. Where partial slits were provided, the rate of increase in the amount of energy absorbed was greater in the case of $\eta = 0.2$ than in the case of $\eta = 0.1$.

Where there were no slits, the energy absorption performance in the case of $\eta = 0.2$ was 0.5 times less than that in the case of $\eta = 0.1$. Where slits were provided, the energy absorption performance in the case of $\eta = 0.2$ was 0.67 times less than and 1.04 times greater than that in the case of $\eta = 0.1$ where $pw = 0.10\%$ and $pw = 0.26\%$, respectively.

(5) Examination of the ultimate strength

Table 4 compares the test and calculation results for the ultimate strength in the case of $\eta = 0.2$, as well as the existing joint strength formulae. The ultimate strength was assumed to be shear where there were no slits, and to be bending where slits were provided. The effective internal height of the columns was set at h_{0e}, which was given various values here. The following insights were obtained from these comparative studies:

With regard to the specimens without slits, the test and calculated values were approximately consistent in the rigid zone in the case of (3) h_{0e} = 520mm, where the reduction rate of shear strength due to torsion stress induced by the eccentricity of wall-column alignment was taken into account. The failure mode predicted from the calculation results were also found approximately consistent with the test results.

With regard to the specimens having slits, the test results were 0.70 to 0.80 times and 1.04 to 1.17 times less than the calculation results in the case of (4) h_{0e} = 680mm and (5) h_{0e} = 1000mm, respectively. It is indicated that the specimens showed a similar behavior to that of independent columns where partial slits were provided.

The joint strength formulae were both approximately consistent with the test results. The formula by Hiraishi yielded a smaller value than the test results, due to its assumption that the column strength was greater than the joint strength. The formula by Shioya yielded a value close to the test results, as it assumes the maximum load that has not caused any failure other than the bending yield of column top and base and joint failure.

Table4 Comparison the test and calculation results (CHW series)

No.	$_tQ_m$ (kN)	R_m (rad.)	Calculation of ultimate strength※1										Slit strength formula	
			Bending $_cQ_{mu}$ (kN)					Shear $_cQ_{su}$ (kN)						
			①	②※2	③※3	④※4	⑤	①	②※2	③※3	④※4	⑤	by Hiraishi※6	by Shioya※7
			T/C	T/C	T/C	T/C	T/C	T/C	T/C	T/C	T/C	T/C	T/C	T/C
11	135.2	3.47	0.39		0.57		1.10	0.60 (0.95)		0.77 (1.17)		1.14 (1.67)		
12	127.1	9.96	0.39	0.53	0.56	0.74	1.08	0.60	0.73	0.76	0.90	1.13	1.15	0.97
13	125.0	4.61	0.38		0.55		1.05	0.55 (0.82)		0.69 (1.01)		0.99 (1.42)		
14	121.7	9.83	0.37	0.50	0.54	0.70	1.04	0.54	0.65	0.68	0.79	0.97	1.10	0.93

note) T: test value(Plus Loading), T/C: (Test value)÷(Calculation value)

$_tQ_m$: Maximum Share force of test value, R_m: Distortion angle at maximum share force

①～⑤ are internal dimensions. (①=360mm, ②=487mm, ③=520mm, ④=680mm, ⑤=1000mm)

Share ultimate strength: $_cQ_{su}$ The value in parenthesis is $_cQ_{st}$※5.

※1 Ultimate strength

・Bending ($_cQ_{mu}$): $_cM_u = 0.5a_g \cdot \sigma_y \cdot g \cdot D_c + 0.5 \cdot N \cdot D_c\left(1 - \frac{N}{b \cdot D \cdot \sigma_B}\right) \rightarrow {}_cQ_{mu} = \frac{2 \times M_u}{h_{0e}}$

・Shear ($_cQ_{su}$): $_cQ_{su} = \left\{\frac{0.12k_u.k_p(180+\sigma_B)}{M/(Q \cdot d)+0.12} + 2.7\sqrt{p_w.\sigma_{wy}}\right\} b \cdot j + 0.1N$

※2 From the reference 2) ② $h_{0e} = h_0 + \sum x$, $x = -(L-h_s) + \sqrt{(L-h_s)^2 + j/a}$

※3 From the reference 3) ③ $h_{0e} = h_0 + 2 \times D_c/3$

※4 From the reference 4) ④ $h_{0e} = h_0 + h_{sw}/s + h_{hw}/s$, $s = t_w/t_d$ (h_{sw}: spandrel wall height, h_{hw}: hanging wall height)

※5 From the reference 5)

$$Q_{ct} = \beta_{ct} \cdot Q_{cu} \qquad \beta_{ct} = \left\{1 + \left(e1\frac{K_{cu}}{K_{cT}}\right)^2\right\}^{-0.5}$$

※6 From the reference 6) Slit joint strength: $C = 0.65 \cdot t \cdot h_s \cdot F_c$

※7 From the reference 7) Slit joint strength: Max((1), (2)) $Q_{SLU} = (Ai \cdot_{SL} \delta_B + \delta_W)\omega + Bi \cdot m + \lambda \cdot M_{CT}$ [illegible] (1) $Q_{SLY} = (M_{CT} + M_{CBY})/h + M_{WBY}/h$ (2)

4. SUMMARY OF TEST RESULTS

The present study experimentally explored the impacts of such factors as the axial force ratio, eccentricity of column-wall joints, amount of column hoops and presence of structural slits, as part of research on the seismic performance of reinforced concrete short columns having non-structural walls, which have been found vulnerable in past earthquake damage examples. As a result, the following insights were gained:

Presence of slits: Regardless of the type of the walls attached, the provision of slits significantly improved both the critical deformation (F) and limit vertical load-bearing capacity (F_u) against horizontal load. For the columns with hanging/podium walls in particular, the energy absorption capacity was also significantly enhanced.

The Phase-I and Phase-II (p_w) comparison: The columns with $p_w = 0.26\%$ showed a greater critical deformation (F) and limit vertical load-bearing capacity (F_u) than those with pw=0.1%. However, the effect of slits were more obvious in the case of $p_w = 0.26\%$.

Difference in the axial force (30kgf/cm^2 and 60kgf/cm^2): The greater the axial force, the smaller the critical deformation (F) and limit vertical load-bearing capacity (F_u). The presence of slits improved F_u to a greater extent where the axial force was larger.

Influence of eccentricity: Attaching non-structural walls on an eccentric alignment with the column axis decreased the maximum strength and resulted in the earlier separation of walls from columns where structural slits were provided.

REFERENCES

1) HIROSAWA Masaya, KOMURO Tatsuya, etc., Failure Mode and Deformation Performance of Short Reinforced Concrete Columns with Non-Structural Walls, EEC final research report, 2006.3.
2) AIJ (Architectural Institute of Japan) (1998.10), Recommendation to RC Structural Design After Hanshin-Awaji Earthquake Disaster : Cause of particularly noticed damages and corresponding RC structural design details
3) Japan Association for Building Research Promotion (2003.3), Seismic Evaluation & Seismic Retrofit Design Manual of Existing Building (2003 edition)
4) KOMURO Tatsuya : Study on the seismic performance evaluation and seismic improvement of existing RC and SRC buildings, Doctor thesis, 2004.3.31
5) HIRAISHI Hisahiro, etc.(1986.4), Study on Effect of Slit on Reinforced Concrete Column-Spandrel Wall Assemblage, *Journal of structural and construction engineering. Transactions of AIJ No. 362*, pp83-91
6) SHIOYA Shinichi (1993.7), Study on Characteristic of Reinforced Concrete Spandrels- Beams-Columns Typed Frames with Structural Slits : Part IV Evaluation of Maximum Lateral Load and Displacement and Failure Mode of Spandrel-columns, *Journal of structural and construction engineering. Transactions of AIJ No. 449*, pp163-173
7) AIJ (1987.9), Data for Ultimate Strength Design of Reinforced Concrete Structures